Inorganic Chemistry

Cyclam-Based "Clickates": Homogeneous and Heterogeneous Fluorescent Sensors for Zn(II)

Emiliano Tamanini,[†] Kevin Flavin,[†] Majid Motevalli,[†] Silvia Piperno,[‡] Levi A. Gheber,[‡] Matthew H. Todd,*[,§] and Michael Watkinson*[,†]

[†]*The Joseph Priestly Building, School of Biological and Chemical Sciences, Queen Mary University of London, Mile End Road, London, E1 4NS, U.K.,* [‡]*Department of Biotechnological Engineering, Ben Gurion University Negev, IL-84105 Beer Sheva, Israel, and* [§]*School of Chemistry, University of Sydney, NSW 2006, Australia*

Received October 2, 2009

In an effort to improve upon the recently reported cyclam based zinc sensor **1**, the "click"-generated 1,8-disubstituted analogue **2** has been prepared. The ligand shows a 2-fold increase in its fluorescence emission compared to **1** exclusively in the presence of Zn(II) that is typical of switch-on PET fluorescent sensors. Single crystal X-ray diffraction of complexes of model ligand **10** reveals that the configuration adopted by the macrocyclic framework is extremely sensitive to the metal ion to which it coordinates. For Zn(II), Mg(II), and Li(I) the metal ions adopt an octahedral geometry with a *trans* III configuration of the cyclam ring. In contrast for Ni(II) the ligand adopts the rare *cis* V configuration, while for Cu(II) a clear preference for five-coordinate geometry is displayed with a *trans* I configuration of the macrocyclic ring being observed in two essentially isostructural compounds prepared via different routes. The ligand displays an increased selectivity for Zn(II) compared to **1** in the majority of cases with excellent selectivity upheld over Na(I), Mg(II), Ca(II), Mn(II), Ni(II), Co(II), and Fe(III). In contrast for Cu(II) and Hg(II) little improvement was observed for **2** compared to **1** and for Cd(II) the selectivity of the new ligand was inferior. In the light of these findings and the slower response times for ligand **2**, our original "click"-generated cyclam sensor system **1** was employed in a proof of concept study to prepare a heterogeneous sol−gel based material which retains its PET response to Zn(II). The versatile nature of the sol−gel process importantly allows the simple preparation of a variety of nanostructured materials displaying high surface area-volume ratio using fabrication methods such as soft lithography, electrospinning, and nanopipetting.

Introduction

Because of the essential and varied role of metal cations in biological systems, allied to concerns over the role of certain elements as environmental pollutants, much effort has focused in recent years on the development of effective sensors for a number of these ions.[1] Arguably greatest interest has focused on the development of sensors for the detection of zinc(II).[2] This reflects the fact that zinc is the second most abundant transition metal in the human body. Although over 90% of zinc is classified as "static", playing crucial structural roles in transcription factors and related proteins, structural

and catalytic roles in enzymes as well as its important role in neural signal transmission, "mobile" pools of zinc exist in certain mammalian organs such as the brain and pancreas, which are carefully regulated. Unsurprisingly it is increasingly recognized that the disruption of these pools of zinc is associated with a number of disease states which include type I and II diabetes,[3] neural function,[4] particularly Alzheimer's disease[5] and certain cancers.[6] Furthermore, zinc is now recognized as an important factor in the regulation of apoptosis.[7] Consequently much effort has been directed toward the preparation of highly specific sensors for the

*To whom correspondence should be addressed. E-mail: m.todd@chem.usyd.edu.au (M.H.T.), m.watkinson@qmul.ac.uk (M.W.).
(1) Domaille, D. W.; Que, E. L.; Chang, C. J. *Nat. Chem. Biol.* **2008**, *4*, 168–175.
(2) (a) Gunnlaugsson, T.; Glynn, M.; Tocci, G. M.; Kruger, P. E.; Pfeffer, F. M. *Coord. Chem. Rev.* **2006**, *250*, 3094–3117. (b) Callan, J. F.; de Silva, A. P.; Magri, D. C. *Tetrahedron* **2005**, *61*, 8551–8588. (c) Carol, P.; Sreejith, S.; Ajayaghosh, A. *Chem. Asian J.* **2007**, *2*, 338–348. (d) Kikuchi, K.; Komatsu, K.; Nagano, T. *Curr. Opin. Chem. Biol.* **2004**, *8*, 182–191. (e) Lim, N. C.; Freake, H. C.; Brückner, C. *Chem.—Eur. J.* **2005**, *11*, 38–49. (f) Nolan, E. M.; Lippard, S. J. *Acc. Chem. Res.* **2009**, *42*, 193–203.

(3) (a) Sladek, R.; et al. *Nature* **2007**, *445*, 881–885. (b) Chimienti, F.; Devergnas, S.; Pattou, F.; Schuit, F.; Garcia-Cuenca, R.; Vandewalle, B.; Kerr-Conte, J.; Van Lommel, L.; Grunwald, D.; Favier, A.; Seve, M. *J. Cell. Sci.* **2006**, *119*, 4199–4206.
(4) Que, E. L.; Domaille, D. W.; Chang, C. J. *Chem. Rev.* **2008**, *108*, 1517–1549.
(5) Frederickson, C. J.; Koh, J. Y.; Bush, A. I. *Nat. Rev. Neurosci.* **2005**, *6*, 449–462.
(6) For example, see: Costello, L. C.; Franklin, R. B.; Feng, P.; Tan, M.; Bagasra, O. *Cancer Cause Control* **2005**, *16*, 901–915.
(7) Zalewski, P. D.; Forbes, I. J.; Betts, W. H. *Biochem. J.* **1993**, *296*, 403–408.
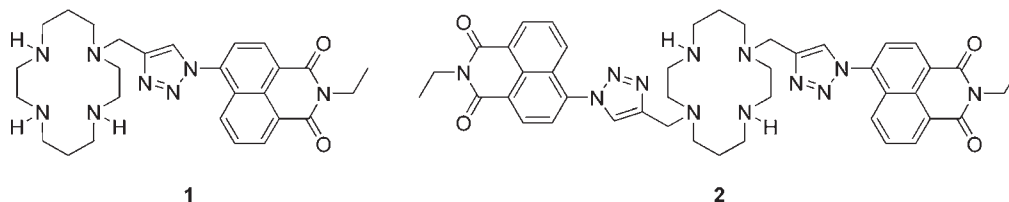
Figure 1. Click-generated fluorescent probes for Zn(II).

detection of Zn(II) both in cellular media and in vivo.[2,8] The vast majority of the sensors reported to date have focused on imaging the spectroscopically silent d[10] ion by preventing fluorophore quenching by photoinduced electron transfer (PET).[9] This is because upon coordination of the functionalized ligand to the metal ion fluorescence is switched on (since the quenching mechanism is turned off) which allows the rapid and facile visualization of this elusive metal ion in biological samples. While many sensors for Zn(II) have been reported, there continues to be extensive interest in the field.[10] This is because the need remains for highly selective, non-toxic, and water-soluble sensors able to operate at physiological pH, which are also able to sense and quantify zinc levels over the broad concentration range known to be present in biology.

Our recent interests in sensing have focused on the use of macrocyclic based ligand systems.[11] While oxygen rich macrocycles have mainly found use as ligands for alkali and alkali earth metals, azamacrocycles are more suited toward coordinating the softer transition metals. Among the azamacrocycles, cyclen is probably the most used for this purpose, and it has proven to be a good ligand in a number of PET-based probes for the zinc ion.[12] Surprisingly, there are very few examples of analogous small molecule cyclam-based fluorescent sensors for Zn(II) that have been shown to display selectivity for zinc.[13] We recently reported the synthesis of the cyclam-based fluorescent Zn(II) sensor **1** (Figure 1), which was easily assembled via the Cu(I)-mediated Huisgen [3 + 2] "click" cycloaddition between a propargyl-functionalized cyclam ionophore and an azide-functionalized naphthalimide fluorophore.[11a] While the "click" reaction has attracted increasing interest in recent years because of its potency in the effective and facile "ligation" of different chemical moieties, the resultant triazole has generally only been used as a junction in the final structures.[14] More recently, however, several systems have appeared in which the heterocycle plays an active role in the functionality of the final product;[11a,b,14g−14i,15]

(8) See for example: (a) Parkesh, R.; Lee, T. C.; Gunnlaugsson, T. *Org. Biomol. Chem*. **2007**, *5*, 310–317. (b) Wang, J.; Xiao, Y.; Zhang, Z.; Qian, X.; Yang, Y.; Xu, Q. *J. Mater. Chem*. **2005**, *15*, 2836–2839. (c) Huang, S.; Clark, R. J.; Zhu, L. *Org. Lett*. **2007**, *9*, 4999–5002. (d) Liu, Y.; Zhang, N.; Chen, Y.; Wang, L.-H. *Org. Lett*. **2007**, *9*, 315–318. (e) Bencini, A.; Berni, E.; Bianchi, A.; Fornasari, P.; Giorgi, C.; Lima, J. C.; Lodeiro, C.; Melo, M. J.; Seixas de Melo, J.; Jorge Parola, A.; Pina, F.; Pina, J.; Valtancoli, B. *Dalton Trans*. **2004**, 2180–2187. (f) Zhang, X.; Lovejoy, K. S.; Jasanoff, A.; Lippard, S. J. *Proc. Natl. Acad. Sci. U.S.A*. **2007**, *104*, 10780–10785. (g) Nolan, E. M.; Jaworski, J.; Okamoto, K. I.; Hayashi, Y.; Sheng, M.; Lippard, S. J. *J. Am. Chem. Soc*. **2005**, *127*, 16812–16823. (h) Tomat, E.; Nolan, E. M.; Jaworski, J.; Lippard, S. J. *J. Am. Chem. Soc*. **2008**, *130*, 15776–15777. (i) Zhang, X.-a.; Hayes, D.; Smith, S. J.; Friedle, S.; Lippard, S. J. *J. Am. Chem. Soc*. **2008**, *130*, 15788–15789. (j) Wong, B. A.; Friedle, S.; Lippard, S. J. *J. Am. Chem. Soc*. **2009**, *131*, 7142–7152.

(9) (a) de Silva, A. P.; Gunaratne, H. Q. N.; Gunnlaugsson, T.; Huxley, A. J. M.; McCoy, C. P.; Rademacher, J. T.; Rice, T. E. *Chem. Rev*. **1997**, *97*, 1515–1566. (b) Valeur, B.; Leray, I. *Coord. Chem. Rev*. **2000**, *205*, 3–40. (c) Prodi, L.; Bolletta, F.; Montaldi, M.; Zaccheroni, N. *Coord. Chem. Rev*. **2000**, *205*, 59–83.

(10) For some examples of recently reported PET Zn sensors see: (a) Majzoub, A. E.; Cadiou, C.; Déchamps-Olivier, I.; Chuburu, F.; Aplincourt, M.; Tinant, B. *Inorg. Chim. Acta* **2009**, *362*, 1169–1178. (b) Liu, Z.; Zhang, C.; Li, Y.; Wu, Z.; Qian, F.; Yang, X.; He, W.; Gao, X.; Guo, Z. *Org. Lett*. **2009**, *11*, 795–798. (c) Xu, Z.; Kim, G.-H.; Han, S. J.; Jou, M. J.; Lee, C.; Shin, I.; Yoon, J. *Tetrahedron* **2009**, *65*, 2307–2312. (d) Li, H.-Y.; Gao, S.; Xi, Z. *Inorg. Chem. Commun* **2009**, *12*, 300–303. (e) Qian, F.; Zhang, C.; Zhang, Y.; He, W.; Gao, X.; Hu, P.; Guo, Z. *J. Am. Chem. Soc*. **2009**, *131*, 1460–1468. (f) Taki, M.; Watanabe, Y.; Yamamoto, Y. *Tetrahedron Lett*. **2009**, *50*, 1345–1347. (g) Xue, L.; Liu, C.; Jiang, H. *Chem. Commun*. **2009**, 1061–1063. (h) Hung, H.-C.; Cheng, C.-W.; Ho, I.-T.; Chung, W.-S. *Tetrahedron Lett*. **2009**, *50*, 302–305. (i) Xue, L.; Liu, C.; Jiang, H. *Org. Lett*. **2009**, *11*, 1655–1658. (j) Khan, F. A.; Parasuraman, K.; Sadhu, K. K. *Chem. Commun*. **2009**, 2399–2401. (k) Xue, L.; Liu, Q.; Jiang, H. *Org. Lett*. **2009**, *11*, 3454–3457. (l) Mizukami, A.; Okada, S.; Kimura, S.; Kikuchi, K. *Inorg. Chem*. **2009**, *48*, 7630–7636. (m) Chen, X.-Y.; Shi, J.; Li, Y.-M.; Wang, F.-L.; Wu, X.; Guo, Q.-X.; Liu, L. *Org. Lett*. **2009**, *11*, 4426–4429. (n) Hanaoka, K.; Muramatsu, Y.; Urano, Y.; Terai, T.; Nagano, T. *Chem. Eur. J*. **2010**, *16*, 568–572. (o) Xu, Z.; Baek, K.-H.; Kim, H. N.; Cui, J.; Qian, X.; Spring, D. R.; Shin, I.; Yoon, J. *J. Am. Chem. Soc*. **2010**, *132*, 601–610. (p) Zhou, Y.; Kim, H. N.; Yoon, J. *Bioorg. Med. Chem. Lett*. **2010**, *20*, 125–128. (q) Ohshima, R.; Kitamura, M.; Morita, A.; Shiro, M.; Yamada, Y.; Ikekita, M.; Kimura, E.; Aoki, S. *Inorg. Chem*. **2010**, *49*, 888–899.

(11) (a) Tamanini, E.; Katewa, A.; Sedger, L. M.; Todd, M. H.; Watkinson, M. *Inorg. Chem*. **2009**, *48*, 319–324. (b) Tamanini, E.; Rigby, S. E. J.; Motevalli, M.; Todd, M. H.; Watkinson, M. *Chem.—Eur. J*. **2009**, *15*, 3720–3728. (c) Krivickas, S. J.; Tamanini, E.; Todd, M. H.; Watkinson, M. *J. Org. Chem*. **2007**, *72*, 8280–8289.

(12) See for example: (a) Kimura, E.; Aoki, S.; Kikuta, E.; Koike, T. *Proc. Natl. Acad. Sci., U.S.A*. **2003**, *100*, 3731–3736. (b) Carol, P.; Sreejith, S.; Ajayaghosh, A. *Chem. Asian J*. **2007**, *2*, 338–348. (c) Akkaya, E. U.; Huston, M. E.; Czarnik, A. W. *J. Am. Chem. Soc*. **1990**, *112*, 3590–3593. (d) Koike, T.; Watanabe, T.; Aoki, S.; Kimura, E.; Shiro, M. *J. Am. Chem. Soc*. **1996**, *118*, 12696–12703. (e) Aoki, S.; Kaido, S.; Fujioka, H.; Kimura, E. *Inorg. Chem*. **2003**, *42*, 1023–1030. (f) El Majzoub, A.; Cadiou, C.; Déchamps-Olivier, I.; Chuburu, F.; Aplincourt, M. *Eur. J. Inorg. Chem*. **2007**, 5087–5097. (g) Aoki, S.; Sakurama, K.; Matsuo, N.; Yamada, Y.; Takasawa, R.; Tanuma, S.; Shiro, M.; Takeda, K.; Kimura, E. *Chem.—Eur. J*. **2006**, *12*, 9066–9080. (h) Hirano, T.; Kikuchi, K.; Urano, Y.; Higuchi, T.; Nagano, T. *Angew. Chem., Int. Ed*. **2000**, *39*, 1052–1054.

(13) (a) Moore, E. G.; Bernhardt, P. V.; Fürstenberg, A.; Riley, M. J.; Smith, T. A.; Vauthey, E. *J. Phys. Chem. A* **2005**, *109*, 3788–3796. (b) Fabbrizzi, L.; Foti, F.; Licchelli, M.; Maccarini, P.; Sacchi, D.; Zema, M. *Chem.—Eur. J*. **2002**, *8*, 4965–4972. (c) Park, S. M.; Kim, M. H.; Choe, J.-I.; No, K. T.; Chang, S.-K. *J. Org. Chem*. **2007**, *72*, 3550–3553. (d) Saudan, C.; Balzani, V.; Gorka, M.; Lee, S.-K.; Maestri, M.; Vicinelli, V.; Vögtle, F. *J. Am. Chem. Soc*. **2003**, *125*, 4424–4425.

(14) (a) Kolb, H. C.; Finn, M. G.; Sharpless, K. B. *Angew. Chem., Int. Ed*. **2001**, *40*, 2004–2021. (b) Whiting, M.; Muldoom, J.; Lin, Y.-C.; Silverman, S. M.; Lindstrom, W.; Olson, A. J.; Kolb, H. C.; Finn, M. G.; Sharpless, K. B.; Elder, J. H.; Fokin, V. V. *Angew. Chem., Int. Ed*. **2006**, *45*, 1435–1439. (c) James, A. L.; Tirrel, D. A. *J. Am. Chem. Soc*. **2003**, *125*, 11164–11165. (d) Wang, Q.; Chang, T. R.; Hilgraf, R.; Fokin, V. V.; Sharpless, K. B.; Finn, M. G. *J. Am. Chem. Soc*. **2003**, *125*, 3192–3193. (e) Lutz, J.-F. *Angew. Chem., Int. Ed*. **2007**, *46*, 1018–1025. (f) Fournier, D.; Hoogenboom, R.; Schubert, U. S. *Chem. Soc. Rev*. **2007**, *36*, 1369–1380. (g) Chan, T. R.; Hilgraf, R.; Sharpless, K. B.; Fokin, V. V. *Org. Lett*. **2004**, *4*, 2853–2855. (h) Dai, Q.; Gao, W.; Liu, D.; Kapes, L. M.; Zhang, X. *J. Org. Chem*. **2006**, *71*, 3928–3934. (i) Detz, R. J.; Heras, S. A.; de Gelder, R.; N. M. van Leeuwen, P. W.; Hiemstra, H.; Reek, J. N. H.; van Maarseveen, J. H. *Org. Lett*. **2006**, *8*, 3227–3230. (j) Luo, S.; Xu, H.; Mi, X.; Li, J.; Zheng, X.; Cheng, J.-P. *J. Org. Chem*. **2006**, *71*, 9244–9248. (k) Moorhouse, A. D.; Moses, J. E. *Chem. Med. Chem*. **2008**, *3*, 715–723. (l) Tron, G. C.; Pirali, T.; Billington, R. A.; Canonico, P. L.; Sorba, G.; Genazzani, A. A. *Med. Res. Rev*. **2008**, *28*, 278–308.

(15) (a) Mindt, T. L.; Struthers, H.; Brans, L.; Anguelov, T.; Schweinsberg, C.; Maes, V.; Tourwé, D.; Schibil, R. *J. Am. Chem. Soc*. **2006**, *128*, 15096–15097. (b) Huang, S.; Clark, R. J.; Zhu, L. *Org. Lett*. **2007**, *24*, 4999–5002. (c) Chang, C.-K.; Su, I.-H.; Senthilvelan, A.; Chung, W.-S. *Org. Lett*. **2007**, *17*, 3363–3366. (d) Jauregui, M.; Perry, W. S.; Allain, C.; Vidler, L. R.; Willis, M. C.; Kenwright, A. M.; Snaith, J. S.; Stasiuk, G. J.; Lowe, M. P.; Faulkner, S. *Dalton Trans*. **2009**, 6283–6285.

in the case of **1** serving as a scorpionate ligand reminiscent of the histidine ligands that bind zinc ions in the active site of a range of enzymes such as carbonic anhydrase. Our papers were the first to report the synthesis of azamacrocycles bearing pendant triazole motifs. In the absence of metal ions the fluorescence of **1** was quenched via PET from the azamacrocycle receptor to the excited state of the naphthalimide fluorophore (Figure 1). On addition of Zn(II) PET was inhibited resulting in a typically strong switch-on enhancement of the fluorescent emission. The sensor upheld excellent selectivity over a range of biologically relevant metal ions including Na(I), Ca(II), Mg(II), and Fe(III), although full fluorescence response was never recovered, and the system was unable to detect zinc in the presence of an excess of either Cu(II) or Hg(II). This system also proved to be cell-permeable and capable of detecting biologically available zinc in mammalian cells, sensing the Zn(II) flux that exists during apoptotic cell death without the need for the addition of extracellular Zn(II).

We envisaged that the performance of **1** could be improved through the development of new "clickates" integrating more than one triazole within the macrocyclic framework. Besides the inherent novelty of these triazole-appended azamacrocycles as architectures for coordination chemistry, the modularity of the click reaction allows for a range of systematic changes to be readily made to the ligand structure, for example, (i) the incorporation of two different fluorophores within the same ligand might allow ratiometric sensing; (ii) the generation of an excimer emission through the interaction of two fluorophores (vide infra), or (iii) the incorporation of two identical fluorophores to increase the intensity of the fluorescence response of the original sensor. We initially targeted the last of these through the second generation fluorescent Zn(II) probe **2**, which presents two identical fluorophores "clicked" onto diametrically opposed cyclam nitrogens. This ligand should preferentially accommodate cations in an octahedral environment with the click-generated triazoles occupying the metal's axial positions when the cyclam ring adopts the thermodynamically favored *trans* (III) geometry.[16] Although it is well established that the stability constants of cyclam ligands of this type with sterically undemanding pendant arms are higher for Cu(II) over Zn(II),[16b,c] we hoped that the larger triazole appended fluorophores in **2** might also provide a kinetic barrier to prevent the coordination of copper over zinc should significant conformational rearrangement of the ligand be required upon metal binding. Although competitive quenching of fluorescence by Cu(II) is a problem for putative zinc sensors in vitro,[10,11a] it is not of general biological relevance as it has been estimated that intracellular free Cu(II) is limited to less than one free copper ion per cell,[17a] although high concentrations of both Cu(II) and Zn(II) can occur in biology, for example, in amyloid plaques.[17b]

Experimental Section

General Information. All reagents were purchased from Sigma-Aldrich and used without further purification. All reac-

(16) (a) Bosnich, B.; Poon, C. K.; Tobe, M. L. *Inorg. Chem.* **1965**, *4*, 1102–1108. (b) Lukěs, I.; Kotek, J.; Vojtíšek, P.; Hermann, P. *Coord. Chem. Rev.* **2001**, *216−217*, 287–312. (c) Kotek, J.; Lubal, P.; Hermann, P.; Císařová, I.; Lukěs, I.; Godula, T.; Svobodová, I.; Táborský, P.; Havel, J. *Chem.—Eur. J.* **2003**, *9*, 233–248.
(17) (a) Rae, T. D.; Schmidt, P. J.; Pufahl, R. A.; Culotta, V. C.; O'Halloran, T. V. *Science* **1999**, *284*, 805–808. (b) Sarell, C. J.; Syme, C. D.; Rigby, S. E. J.; Viles, J. H. *Biochemistry* **2009**, *48*, 4388−4402 and references cited therein.

tions were carried out using commercial grade solvents. Flash chromatography was carried out using BDH silica gel. ^{1}H and ^{13}C NMR spectra were recorded on a JEOL JMN-EX270 NMR spectrometer at 270 and 67.5 MHz respectively. ^{1}H chemical shifts are reported in parts per million (ppm) relative to the residual proton signal of the deuterated solvents. Coupling constants (J) are reported in hertz (Hz). ^{13}C chemical shifts are reported in parts per million relative to the carbon signal of the solvents. IR spectra were recorded with a Shimadzu FTIR-8300. Fluorescence emission spectra were recorded with a Jobin Yvon Horiba FluoroMax-3 in a 1 cm path length cell. Electrospray Ionization mass spectroscopy was obtained from the EPSRC National Mass Spectrometry Service, University of Wales, Swansea with either a Waters ZQ400 or a Micromass Quattro II. Accurate masses were recorded with either a Finnigan MAT900 or MAT 95 using polyethylenimine as reference.

1,8-Di-prop-2-ynyl-1,4,8,11-tetraaza-tricyclo[9.3.1.1^{4,8}]hexadecane Bromide Salt (4). To a solution of **3**[18] (556 mg, 2.5 mmol) in acetonitrile (50 mL) was added propargyl bromide (80% in toluene, 1.4 mL, 12.4 mmol), and the reaction mixture was stirred at room temperature (rt) overnight. The white precipitate formed was filtered, washed with cold acetonitrile, and dried in vacuo to give the desired product **4** as a white powder (926 mg, 78% yield): mp = 102−104 °C; ^{1}H NMR (D$_2$O): δ 5.48−5.36 (m, 2n), 4.83 (s, 1n), 4.58−4.28 (m, 6n), 3.92−3.76 (m, 2n), 3.70−3.24 (m, 12n), 3.22−3.06 (m, 2n), 3.00−2.80 (m, 4n), 2.72−2.38 (m, 4n), 2.06−1.86 (m, 3n); the presence of different conformers and possibly diastereoisomers in solution makes it difficult to assign the multiplicity and the integral values in the ^{1}H NMR. The integrals are reported as "n" which represents the proportion between the integrals of different signals in the spectrum (see Supporting Information);
^{13}C NMR (D$_2$O): δ 82.5, 82.0, 77.8, 76.4, 75.9, 70.0, 61.3, 53.1, 51.3, 51.0, 50.3, 48.5, 47.2, 45.1, 40.8, 21.9, 19.8; MS (ESI) m/z: 381 [(M − Br)$^+$], 151 [(M − 2Br)$^{2+}$]; HRMS (ES) calcd. for C$_{18}$H$_{30}$N$_4$^{79}Br [(M − Br)$^+$] 381.1648, found. 381.1644.

1,8-Di-prop-2-ynyl-1,4,8,11tetraaza-cyclotetradecane (5). To the bisaminal intermediate **4** (926 mg, 1.9 mmol) was added 3 M NaOH (80 mL), and the resulting suspension was stirred at rt for 3 h. The product was extracted with CH$_2$Cl$_2$ (3 × 60 mL), the combined organic phases were dried (MgSO$_4$) and concentrated in vacuo to afford the desired product **5** as a colorless glue in quantitative yield (540 mg); ν_{max}(CH$_2$Cl$_2$)/cm^{-1}: 3302, 2134; ^{1}H NMR (CDCl$_3$): δ 3.40 (d, J = 2.2, 4H), 2.90−2.50 (m, 18H), 2.14−2.80 (m, 2H), 1.75−1.62 (m, 4H); ^{13}C NMR (CDCl$_3$): δ 78.1, 72.9, 53.9, 51.3, 49.8, 47.1, 41.2, 25.7; MS (ESI) m/z: 277.2 [(M+H)$^+$]; HRMS (ES) calcd. for C$_{16}$H$_{29}$N$_4$ [(M+H)$^+$] 277.2387, found. 277.2390.

4,11-Di-prop-2-ynyl-1,4,8,11tetraaza-cyclotetradecane-1,8-dicarboxylic acid Di-*tert*-butyl Ester (6). To a solution of **5** (552 mg, 2.0 mmol) in CH$_2$Cl$_2$ (20 mL) were added TEA (834 μL, 6.0 mmol), di-*tert*-butyl dicarbonate (958 mg, 4.4 mmol) and DMAP (49 mg, 20 mol %), and the reaction mixture was stirred at rt for 16 h. The reaction was quenched by addition of a saturated solution of NaHCO$_3$ (20 mL) and extracted with CH$_2$Cl$_2$ (3 × 50 mL). The combined organic phases were dried (MgSO$_4$) and concentrated in vacuo. The crude material was purified by flash chromatography on silica gel (EtOAc, 100%) to afford pure **6** as a colorless solid (950 mg, 84% yield): mp = 153−155 °C ; ν_{max} (CH$_2$Cl$_2$)/cm^{-1}: 3302, 1678; ^{1}H NMR (CDCl$_3$): δ 3.42−3.20 (m, 12H), 2.68−2.58 (m, 4H), 2.56−2.44 (m, 4H), 2.14 (s, 2H), 1.76−1.60 (m, 4H), 1.43 (s, 18H); ^{13}C NMR (CDCl$_3$): δ 155.8, 79.4, 78.7, 72.8, 52.9, 51.2, 46.5, 43.4,

(18) (a) Royal, G.; Dahaoui-Gindrey, V.; Dahaoui, S.; Tabard, A.; Guilard, R.; Pullumbi, P.; Lecomte, C. *Eur. J. Org. Chem.* **1998**, 1971–1975. (b) Kurosaki, H.; Bucher, C.; Espinosa, E.; Barbe, J.-M.; Guilard, R. *Inorg. Chim. Acta* **2001**, *322*, 145–149.

43.0, 28.5, 26.9; MS (ESI) m/z: 477.3 [(M+H)$^+$]; HRMS (ES) calcd. for $C_{26}H_{45}N_4O_4$ [(M+H)$^+$], 477.3435, found. 477.3435.

4,11-Bis-[1-(2-ethyl-1,3-dioxo-2,3-dihydro-1H-benzo[de]iso-quinolin-6-yl)-1H-[1,2,3]triazol-4-ylmethyl]-1,4,8,11-tetraaza-cyclotetradecane-1,8-dicarboxylic Acid Di-*tert*-butyl Ester (8). To a solution of **6** (174 mg, 375 μmol) in THF/H$_2$O (7/3, 10 mL) were added **7**[11a] (220 mg, 825 μmol), CuSO$_4$·5H$_2$O (9.3 mg, 10 mol %), and sodium ascorbate (15 mg, 20 mol %) under N$_2$. The solution was stirred at rt overnight. Saturated NH$_4$Cl (20 mL) was added, and volatiles were evaporated in vacuo. The aqueous residue was extracted with CH$_2$Cl$_2$ (3 × 30 mL), and the combined organic portions were dried (MgSO$_4$), filtered, and concentrated in vacuo. The crude material was purified by flash chromatography on silica gel (EtOAc: Pet. spirit 9:1 ramping to EtOAc 100%) to give **8** as a yellow solid (234 mg, 62% yield): mp = 142−143 °C; ν_{max} (CH$_2$Cl$_2$)/cm^{-1}: 3054, 1665, 1650; ^{1}H NMR (CDCl$_3$): δ 8.68−8.30 (m, 4H), 8.20−7.86 (m, 4H), 7.84−7.58 (m, 4H), 4.30−4.14 (m, 4H), 3.98−3.76 (m, 4H), 3.60−3.20 (m, 8H), 2.80−2.40 (m, 8H), 2.10−1.60 (m, 4H), 1.50−1.14 (m, 24H); ^{13}C NMR (CDCl$_3$): δ 163.2, 162.7, 155.8, 146.7, 138.9, 131.8, 130.3, 129.4, 128.6, 128.4, 126.2, 125.1, 123.4, 122.7, 79.4, 77.4, 55.1, 52.2, 50.3, 50.1, 47.3, 46.8, 35.7, 28.5, 13.3; MS (ES) m/z: 1009.6 [(M+H)$^+$]; HRMS (ES) calcd. for $C_{54}H_{65}N_{12}O_8$ [(M+H)$^+$], 1009.5043, found 1009.5043.

4,11-Bis-[1-(2-ethyl-1,3-dioxo-2,3-dihydro-1H-benzo[de]isoqui-inolin-6-yl)-1H-[1,2,3]triazol-4-ylmethyl]-1,4,8,11-tetraaza-cyclo-tetradecane (2). To **8** (150 mg, 149 μmol) was added TFA (20% in CH$_2$Cl$_2$, 5 mL) at rt, and the reaction mixture was stirred for 3 h. A saturated solution of NaHCO$_3$ (10 mL) was added, and the product was extracted with CH$_2$Cl$_2$ (3 × 20 mL). The combined organic phases were dried (MgSO$_4$), filtered, and the volatiles were removed in vacuo to give **2** as a yellow solid (107 mg, 89% yield): mp = 95−97 °C; ν_{max} (CH$_2$Cl$_2$)/cm^{-1}: 3054, 1664; ^{1}H NMR (CDCl$_3$): δ 8.62−8.52 (m, 4H), 8.12 (d, J = 8.4, 2H), 8.00 (s, 2H), 7.80−7.68 (m, 4H), 4.18 (q, J = 7.0, 4H), 3.88 (s, 4H), 2.80−2.50 (m, 16H), 1.87 (bs, 4H), 1.27 (t, J = 7.0, 6H); ^{13}C NMR (CDCl$_3$): δ 163.4, 162.9, 144.3, 138.2, 132.0, 130.5, 129.4, 129.0, 128.6, 126.4, 125.2, 123.8, 123.5, 122.9, 53.9, 53.5, 51.8, 49.9, 47.7, 47.5, 35.8, 25.9, 13.3; MS (ESI) m/z: 809.6 [(M+H)$^+$]; HRMS (ES) calcd. for $C_{44}H_{49}N_{12}O_4$ [(M+H)$^+$], 809.3994, found 809.3997.

4,11-Bis-(1-benzyl-1H-[1,2,3]triazol-4-ylmethyl)-1,4,8,11tetra-aza-cyclotetradecane-1,8-dicarboxylic Acid Ditert-butyl Ester (9). To a solution of **6** (200 mg, 420 μmol) in THF/H$_2$O (7/3, 10 mL) were added benzyl azide (115 μL, 924 μmol), Cu-SO$_4$·5H$_2$O (10.5 mg, 10 mol %), and sodium ascorbate (16.6 mg, 20 mol %) under N$_2$. The solution was stirred at rt overnight. Saturated NH$_4$Cl (20 mL) was added, and volatiles were evaporated in vacuo. The aqueous residue was extracted with CH$_2$Cl$_2$ (3 × 30 mL), and the combined organic portions were dried (MgSO$_4$), filtered, and concentrated in vacuo. The crude material was purified by flash chromatography on silica gel (EtOAc: Pet. spirit 9:1 ramping to EtOAc 100%) to give the desired product **9** as a pale yellow solid (280 mg, 90% yield): mp = 60−62 °C; ν_{max} (CH$_2$Cl$_2$)/cm^{-1}: 1678, 1419; ^{1}H NMR (CDCl$_3$): δ 7.42−7.12 (m, 12H), 5.43 (s, 4H), 3.64 (s, 4H), 3.38−3.10 (m, 8H), 2.58−2.46 (m, 4H), 2.42−2.32 (m, 4H), 1.72−1.56 (m, 4H), 1.34 (s, 18H); ^{13}C NMR (CDCl$_3$): δ 155.7, 145.2, 135.0, 129.1, 128.6, 127.9, 122.4, 79.2, 77.4, 53.9, 53.7, 51.9, 50.4, 46.9, 46.5, 28.5, 27.2; MS (ESI) m/z: 743.7 [(M+H)$^+$]; HRMS (ES) calcd. for $C_{40}H_{59}N_{10}O_4$ [(M+H)$^+$], 743.4715, found. 743.4714.

1,8-Bis-(1-benzyl-1H-[1,2,3]triazol-4-ylmethyl)-1,4,8,11-tetra-aza-cyclotetradecane (10). To **9** (280 mg, 377 μM) was added TFA in (20% in DCM, 5 mL), and the reaction mixture was stirred at rt overnight. The reaction was quenched with saturated NaHCO$_3$ solution (10 mL), and the product was extracted with DCM (3 × 30 mL). The combined organic phases were

dried (MgSO$_4$), filtered and concentrated in vacuo to give **10** as a colorless semisolid (178 mg, 87% yield): ν_{max} (CH$_2$Cl$_2$)/cm^{-1}: 3433, 1461, 1358; ^{1}H NMR (CDCl$_3$): δ 7.41 (s, 2H), 7.30−7.10 (m, 10H), 5.40 (s, 4H), 3.59 (s, 4H), 2.74−2.32 (m, 16H), 1.76−1.60 (m, 4H); ^{13}C NMR (CDCl$_3$): δ 144.4, 134.9, 129.0, 128.6, 127.9, 122.8, 53.9, 52.6, 51.6, 49.1, 48.2, 47.0, 25.3; MS (ESI) m/z: 543.5 [(M+H)$^+$]; HRMS (ES) calcd. for $C_{30}H_{43}N_{10}$ [(M+H)$^+$], 543.3667, found 543.3670.

General Procedure for the Synthesis of Metal Complexes with Ligand 10. To a solution of **10** (100 mg, 0.18 mmol) in MeOH (5 mL) was added 1 equiv of the metal ion as a perchlorate salt. The solution was stirred overnight at rt. The solid formed was removed by filtration, washed with a small amount of cold MeOH, and dried in vacuo. Single crystals suitable for X-ray diffraction were obtained by slow diffusion of toluene vapor into a solution of the metal complex in acetonitrile.

[Zn(10)](ClO$_4$)$_2$ was obtained as described above from Zn-(ClO$_4$)·6H$_2$O as a colorless crystal in 62% yield. HRMS (ES) calcd. for $C_{30}H_{42}N_{10}O_4$ClZn (M − ClO$_4$)$^+$, 705.2365, found 705.2361. **[Ni(10)](ClO$_4$)$_2$** was obtained as described above from Ni(ClO$_4$)·6H$_2$O as a pink crystal in 71% yield. HRMS (ES) calcd. for $C_{30}H_{42}N_{10}O_4$ClNi (M − ClO$_4$)$^+$, 699.2427, found 699.2431. **[Cu(10)](ClO$_4$)$_2$** was obtained as described above from Cu(ClO$_4$)·6H$_2$O as deep blue crystals in 80% yield. HRMS (ES) calcd. for $C_{30}H_{42}N_{10}O_4$ClCu (M − ClO$_4$)$^+$, 704.2370, found 704.2370. **[Cu(10)](PF$_6$)$_2$** was obtained as previously described.[21]

6-Bromo-2-(3-hydroxypropyl)-1H-benzo[de]isoquinoline-1,3(2H)-dione (12). To a stirred solution of **11** (500 mg, 1.8 mmol) in dioxane (20 mL) was added 3-aminopropan-1-ol (163 mg, 2.16 mmol), and the solution was heated at reflux overnight under a nitrogen atmosphere. The reaction mixture was cooled to rt, and the product precipitated by the addition of water (40 mL). The precipitate was collected by filtration, washed with water, and dried in vacuo to provide **12** as a gold-yellow solid (416 mg, 70% yield): ν_{max} (CH$_2$Cl$_2$)/cm^{-1} 2307, 1701, 1655, 1419, 1269; ^{1}H NMR (CDCl$_3$): δ 8.57 (d, J = 7.2, 1H), 8.48 (d, J = 8.7, 1H), 8.32 (d, J = 7.9, 1H), 7.96 (d, J = 7.9, 1H), 7.78 (m, 1H), 4.28 (t, J = 6.2, 2H), 3.57 (t, J = 5.4, 2H), 3.06 (bs, 1H), 1.95 (m, 2H); ^{13}C NMR (CDCl$_3$): δ = 164.1 (2 × C═O), 133.4, 132.2, 131.4, 131.1, 130.6, 130.5, 128.8, 128.1, 122.6, 121.7, 58.9, 37.0, 30.9; MS (ESI) m/z: 336.1, 334.1 [(M+H)$^+$ for ^{81}Br and ^{79}Br respectively], 329.2; HRMS (ES) calcd. for $C_{15}H_{13}^{79}$BrNO$_3$ [(M+H)$^+$] 334.0073, found 334.0078.

6-Azido-2-(3-hydroxypropyl)-1H-benzo[de]isoquinoline-1,3(2H)-dione (13). To a stirred solution of **12** (400 mg, 1.19 mmol) in N-pyrrolidinone (6 mL) was added sodium azide (389 mg, 5.98 mmol), and the mixture heated at 110 °C for 1 h. The reaction mixture was cooled to rt, washed with brine, and the organic phase dried (MgSO$_4$). The solvent was removed in vacuo to afford **13** as a dark orange solid (191 mg, 54%): ν_{max} (CH$_2$Cl$_2$)/cm^{-1} 2125, 1697, 1654, 1589, 1419; ^{1}H NMR (CDCl$_3$): δ = 8.57 (dd, J = 7.2, 1.2, 1H), 8.51 (d, J = 7.9, 1H), 8.39 (dd, J = 8.4, 1.2, 1H), 7.70 (dd, J = 8.4, 7.3, 1H), 7.40 (d, J = 7.9, 1H), 4.29 (t, J = 6.2, 2H), 3.56 (t, J = 5.2, 2H), 3.15 (bs, 1H), 1.97−1.92 (m, 2H); ^{13}C NMR (CDCl$_3$): δ = 164.5, 164.1, 143.4, 132.5, 132.0, 129.0, 126.8, 124.2, 122.1, 118.3, 114.7, 58.8, 36.8, 30.9 (presumably because of overlapping signals not all signals were resolved); MS (ESI) m/z: 297.2 [(M+H)$^+$], 256.1, 105.0, 60.3; HRMS (ESI) calcd. for $C_{15}H_{13}N_4O_3$ [(M+H)$^+$] 297.0982, found 297.0978.

Tri-*tert*-butyl-11-((1-(2-(3-hydroxypropyl)-1,3-dioxo-2,3-dihydro-1H-benzo[de]isoquinolin-6-yl)-1H-1,2,3-triazol-4-yl)methyl)-1,4,8,11-tetraazacyclotetradecane-1,4,8-tricarboxylate (15). To a stirred solution of **14** (180 mg, 0.335 mmol) in H$_2$O/THF (3/1, 10 mL) under N$_2$ were added **13** (100 mg, 0.335 mmol), CuSO$_4$·5H$_2$O (4.2 mg, 0.017 mmol), and sodium ascorbate (6.6 mg, 0.033 mmol), and the mixture was stirred overnight. The reaction mixture was quenched with saturated NH$_4$Cl (10 mL), the volatiles were removed in vacuo, and the residue extracted with DCM (3 × 30 mL). The combined organic portions were dried

(MgSO$_4$) and concentrated in vacuo. The crude material was purified by silica gel column chromatography (8/2, EtOAc:Pet. spirit 8:2 ramping to EtOAc:MeOH 9:1) to afford **13** as an orange-yellow solid (280 mg, 64% yield): ν_{max} (CH$_2$Cl$_2$)/cm^{-1}: 3055, 1662, 1647; ^{1}H NMR (CDCl$_3$): δ 8.73−8.70 (m, 2H), 8.36−8.28 (m, 1H), 7.91−7.86 (m, 3H), 4.39−4.35 (m, 2H), 3.95 (m, 2H), 3.65−3.61 (m, 2H), 3.36 (m, 12H), 2.74−2.72 (m, 2H), 2.59−2.55 (m, 2H), 2.03−1.64 (m, 6H), 1.39 (m, 30H); ^{13}C NMR (CDCl$_3$): δ 163.2, 163.6, 155.8, 155.6, 138.5, 132.4, 131.1, 130.0, 129.0, 128.7, 126.4, 125.1, 123.6, 123.4, 122.6, 79.7, 59.2, 47.6, 45.6, 37.3, 31.0, 28.5; MS (ESI) m/z: 835.5 [(M+H)$^+$], 501.4; HRMS (ESI) calcd. for C$_{43}$H$_{63}$N$_8$O$_9$ [(M+H)$^+$] 835.4713, found 835.4707.

6-(4-((1,4,8,11-Tetraazacyclotetradecan-1-yl)methyl)-1*H*-1,2,3-triazol-1-yl)-2-(3-hydroxypropyl)-1*H*-benzo[*de*]isoquinoline-1,3(2*H*)-dione (16). A solution of TFA (20% in DCM, 10 mL) was added to **15** (182 mg, 0.218 mmol), and the reaction mixture was stirred at rt for 2 h. The reaction mixture was quenched with saturated NaHCO$_3$ (10 mL), and the product extracted with CH$_2$Cl$_2$ (3 × 20 mL). The organic layer was dried (MgSO$_4$), filtered and concentrated in vacuo to afford **16** as an orange-yellow solid which was used without further purification (114 mg, 98%): ν_{max} (CH$_2$Cl$_2$)/cm^{-1}: 3055, 1662, 1593; ^{1}H NMR (CDCl$_3$): δ 8.71−8.68 (m, 2H), 8.23−8.20 (m, 1H), 7.98−7.94 (m, 2H), 7.88−7.82 (m, 1H), 4.47 (t, J = 6.2, 1H), 4.35 (t, J = 6.1, 2H), 3.61 (t, J = 5.7, 2H), 3.31−2.88 (m, 14H), 2.30−2.21 (m, 2H), 2.04−1.95 (m, 5H); ^{13}C NMR (CDCl$_3$): δ 164.1, 163.7, 163.6, 163.2, 162.1, 144.6, 138.1, 132.5, 131.0, 129.6, 129.0, 128.8, 126.5, 125.1, 124.4, 123.8, 122.6, 119.0, 114.6, 66.2, 59.2, 56.9, 54.9, 49.3, 49.0, 48.4, 47.9, 47.0, 45.7, 45.5, 37.4, 31.0, 27.0, 25.6, 23.1; MS (ESI) m/z: 535.4 [(M+H)$^+$]; HRMS (ESI) calcd. for C$_{28}$H$_{39}$N$_8$O$_3$ [(M+H)$^+$] 535.3140, found 535.3139.

Preparation of Sol−Gel Based Micro/Nanostructured Materials. Sol−Gel Preparation. Aliquots of 32% HCl (aq) (0.027 mL) and ethanol (5.7 mL) were added to water (0.475 mL). Tetraethoxysilane (TEOS) (1.71 mL) was added slowly to this solution, and the mixture allowed to stir for 10 min. Ligand 16 (10 mg, 0.019 mol) in ethanol (2 mL) was slowly added to the reaction mixture which was then allowed to stir for 24 h. This produced a solution with a molar composition of 1 TEOS: 15 EtOH: 0.1 HCl: 3 H$_2$O while the Si/fluorescent ligand molar ratio was 400.

Preparation of Zinc-Selective Sol−Gel Based Micropattern by Soft Lithography. A polydimethylsiloxane (PDMS) stamp was fabricated using a silicon grid as template. The dimensions of the stamp prepared were 5 μm (micropattern cross-section), spaced 5 μm apart, with a height of 1.2 μm. To produce the microstructure, the stamp was immersed in a drop of the sol solution, and subsequently pressed against a glass substrate (cleaned by immersion in piranha solution, followed by acetone and dried under a stream of nitrogen) for 45 s. The templated substrate was then cured at 80 °C for 12 h following the removal of the stamp.

Preparation of Zinc-Selective Sol−Gel Based Nanofibers. The prepared sol (3 mL) was modified by addition of polyethylene oxide (PEO) (180 mg) to elevate the solution viscosity. For electrospinning, each sol was transferred to a 1 mL syringe and delivered to the stainless steel needle manually. The needle was connected to a high voltage direct current (DC) power supply (Gamma High Voltage Research-ES 20KV). Glass micrsocope slides, wrapped with aluminum foil were used as the counter electrode and mounted at distances between 5 and 15 cm from the needle. Continuous hybrid organic/inorganic nanofibers were electrospun at rt using a driving voltage of 20 kV and collected on the glass substrates, which were subsequently cured at 80 °C for 12 h to remove solvent and stabilize the fibers.

Preparation of Zinc-Selective Sol−Gel Based Microarray. Array deposition on glass substrates was performed under ambient conditions using a Nanonics NSOM/AFM 100 system

(Nanonics, Jerusalem, Israel) with a flat scanner and two coaxial optical microscopes that allowed examination of the sample simultaneously from above and below. Nanofountain pen probes, which are cantilevered nanopipettes (300−600 nm aperture diameter) were used for deposition of single microdots of sol solution on the substrate. Following deposition, microarrays were cured at 80 °C for 12 h to remove solvent and stabilize the structures.

X-ray Crystallography. Data were collected at 120 K using a Nonius Kappa CCD area detector diffractometer mounted at the window of molybdenum rotating anode (50 KV, 90 mA, λ = 0.71069 Å). The crystal-to-detector distance was 30 mm, and ϕ and Ω scans (2.0° increments, 12 s exposure time) were carried out to fill the Ewald sphere. Data collection and processing were carried out using the COLLECT,[33] DENZO,[34] and MaXus[35] softwares, and empirical absorption correction was applied using SORTAV.[36] The structures were solved by heavy-atom method using DIRDIF99,[37] and refined by full-matrix least-squares on F^2 using the SHELXL-97[38] program. All non-hydrogen atoms were refined anisotropically with hydrogen atoms included in idealized positions with thermal parameters riding on those of parent atom (N−H on the cyclam rings were refined freely, except for [Zn(**10**)](ClO$_4$)$_2$ and [Mg(**10**)](ClO$_4$)$_2$ which were idealized). The programs ORTEP-3[39] and PLATON[40] were used for drawing the molecules. WINGX[41] was used to prepare material for publication. All data relating to these single crystal X-ray structures have been deposited at the Cambridge Crystallographic Database: CCDC 730863 ([Cu(**10**)]-(ClO$_4$)$_2$), 730864 ([Cu(**10**)](PF$_6$)$_2$), 730865 ([Li(**10**)](ClO$_4$)$_2$), 730866 ([Mg(**10**)](ClO$_4$)$_2$), 730867 ([Ni(**10**)](ClO$_4$)$_2$), and 730868 ([Zn(**10**)](ClO$_4$)$_2$).

AFM Imaging. AFM images were taken in contact mode using a Nanonics NSOM/AFM 100 system (Nanonics, Jerusalem, Israel) and "Ultrasharp" contact probes from MikroMasch (0.03 N/m nominal spring constant) at ~ 1 Hz line-scan velocity.

Results and Discussion

Ligand Synthesis. The most convenient way to access 1,8-disubstituted cyclam ligands is via the Guilard procedure[18] which allows the facile and completely selective alkylation of the diametrically opposite cyclam nitrogen atoms. The synthesis (Scheme 1) starts from cyclam bis-aminal **3** which is easily obtained by treatment of cyclam with formaldehyde in water following well-known procedures.[19] Treatment of **3** with propargyl bromide in acetonitrile afforded the 1,8-dialkylated product **4** in 78% yield. Removal of the aminal groups was effected in quantitative yield by basic hydrolysis in 3 M NaOH solution. While click reactions have recently been performed on unprotected azamacrocyclic ligands,[15d,20] this requires either prior metalation of the macrocycle or an excess of copper for the reaction to proceed, implying Cu-cyclam complexes formed in situ are inactive catalysts. Consequently we elected to Boc-protect the secondary amine groups to prevent coordination of copper to the azamacrocycle, thus also obviating the need for its subsequent removal. The double click reaction between **6** and azido naphthalimide **7** proceeded smoothly, and the desired product **8** was isolated in 62% yield after

(19) (a) Gabe, E. J.; Le Page, Y.; Prasad, L. *Acta Crystallogr.* **1982**, *B38*, 2752–2754. (b) Bailly, T.; Leroux, Y.; Manouni, E. D.; Neuman, A.; Prange, T.; Burgada, R. *C. R. Acta Sci.* **1996**, Ser IIB, 151−154.
(20) Antoni, P.; Malkoch, M.; Vamvounis, G.; Nyström, D.; Nyström, A.; Lindgren, M.; Hult, A. *J. Mater. Chem.* **2008**, *18*, 2545–2554.
(21) El Ghachtouli, S.; Cadiou, C.; Déchamps-Olivier, I.; Chuburu, F.; Aplincourt, M.; Roisnel, T. *Eur. J. Inorg. Chem.* **2006**, 3472–3481.

Scheme 1. Synthesis of Sensor **2** and Model System **10**[a]
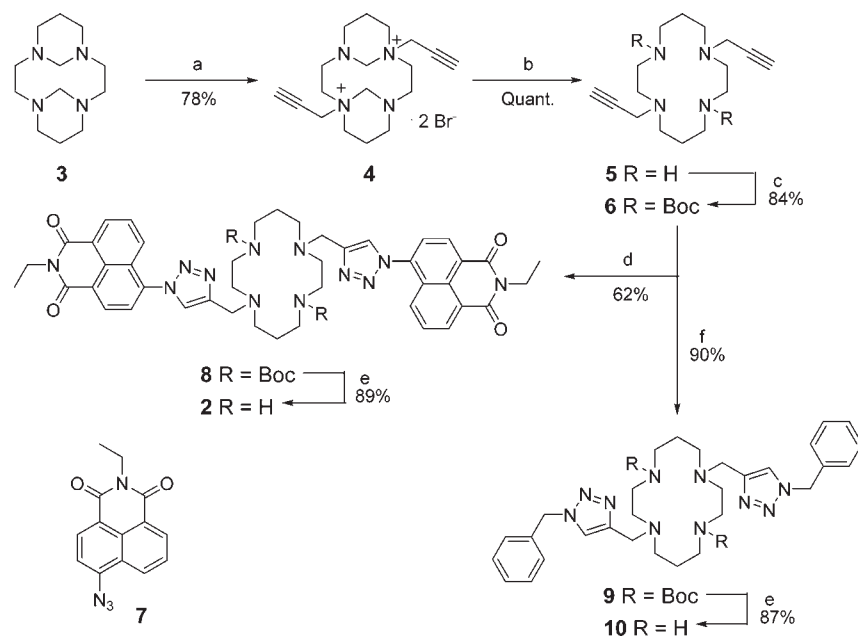
[a] *Reagents and conditions*: (a) Propargyl bromide, CH$_3$CN, rt; (b) 3 M NaOH, rt, 3 h; (c) Boc$_2$O, TEA, cat. DMAP, CH$_2$Cl$_2$; (d) **7**, CuSO$_4$·5H$_2$O (10 mol %), Na ascorbate (20 mol %), H$_2$O/THF, rt; (e) TFA (20% in CH$_2$Cl$_2$); (f) **7**, CuSO$_4$·5H$_2$O (10 mol %), Na ascorbate (20 mol %), H$_2$O/THF, rt.

chromatography. In the final step, Boc protecting groups were readily removed by treatment of **8** with 20% TFA in CH$_2$Cl$_2$ to afford sensor **2** in an excellent yield of 89%. In addition the model "double-click" ligand **10** was also prepared in an analogous manner to investigate the coordination chemistry of the new ligand system, an approach that we have successfully adopted previously.[11a] Thus model ligand **10** was prepared by a double click reaction between Boc-protected cyclam **6** and benzyl azide. Removal of the Boc groups with TFA in CH$_2$Cl$_2$ afforded the desired product **10** in excellent yield (78% over two steps).

Coordination Chemistry of Model Ligand 10. To investigate the coordination geometry of **2** with various metals, complexes of model ligand **10** were prepared by treatment of its methanolic solution with 1 equiv of the perchlorate salt of a number of different metal ions (see Experimental Section). Single crystals suitable for X-ray diffraction were obtained for [Zn(**10**)](ClO$_4$)$_2$, [Ni(**10**)](ClO$_4$)$_2$, and [Cu(**10**)](ClO$_4$)$_2$ by slow vapor diffusion of toluene into acetonitrile solutions of the complexes (Figure 2). In addition we employed a known procedure for synthesis of copper(II) complexes of cyclam in which the macrocycle adopts the trans (III) configuration by the aerial oxidation of a copper(I) complex to give [Cu(**10**)](PF$_6$)$_2$,[21] with crystals suitable for single crystal X-ray diffraction being obtained as before. During these studies we also isolated and crystallographically characterized two other species, [Li(**10**)]ClO$_4$ and [Mg(**10**)](ClO$_4$)$_2$, presumably through adventitious metalation of the macrocycle during the synthesis (see Supporting Information). The crystal structures of the other cationic complexes are presented in Figure 2 together with the crystallographic data in Table 1, and selected bond lengths and angles in Table 2.

We were pleased to see that the configuration adopted by the cyclam ring in the metal complexes varied con-

siderably with three of the five possible configurations being exhibited: the standard and expected[16b,c] *trans* (*I*) configuration with copper(II); the *trans* (*III*) configuration with zinc(II), in which the metal adopts an octahedral coordination geometry with the two triazole rings occupying the opposite axial sites (the magnesium(II) and lithium(I) complexes are essentially isostructural); while for nickel(II) the more unusual *cis* (*V*) configuration was observed.[22] This shows that for copper(II) there is a very clear preference for five coordinate geometry and the *trans* (*I*) configuration of the macrocycle with only one heterocycle chelating the metal even when procedures previously shown to result in complexes with *trans* (*III*) configurations were employed. The structures are intermediate between square based pyramidal and trigonal bipyramidal geometry ($\tau = 0.50$ for [Cu(**10**)](ClO$_4$)$_2$ and 0.49 for [Cu(**10**)](PF$_6$)$_2$)[23] and are comparable to a number of previously reported complexes of this type.[16b,c]

Efficacy of 2 in Zinc Sensing. Given the very different coordination modes exhibited for **10** together with the already high selectivity of **1** for zinc we were optimistic that its analogue **2** would also provide excellent selectivity for zinc over a range of other metal ions. The fluorescence of a 10 μM solution of **2** in H$_2$O/CH$_3$CN (7:3) buffered at pH 7 (50 mM HEPES buffer) showed an emission band at about 416 nm after excitation at 350 nm, mirroring the behavior of the monosubstituted system **1** (Figure 3). Upon addition of 1 equiv of Zn(II) a 12.7-fold increase of the emission maximum was observed. The [1:1] stoichiometry of the complex in solution was confirmed by

(22) (a) Donnelly, M. A.; Zimmer, M. *Inorg. Chem.* **1999**, *38*, 1650–1658. (b) McRobbie, G.; Valks, G. C.; Empson, C. J.; Khan, A.; Silversides, J. D.; Pannecouque, C.; De Clercq, E.; Fiddy, S. G.; Bridgeman, A. J.; Young, N. A.; Archibald, S. J. *Dalton Trans.* **2007**, 5008–5018. (c) Silversides, J. D.; Allan, C. C.; Archibald, S. J. *Dalton Trans.* **2007**, 971–978.

(23) Addison, A. W.; Rao, T. N.; Reddjik, J.; van Rijn, J.; Verschoor, G. C. *J. Chem. Soc., Dalton Trans.* **1984**, 1349–1356.
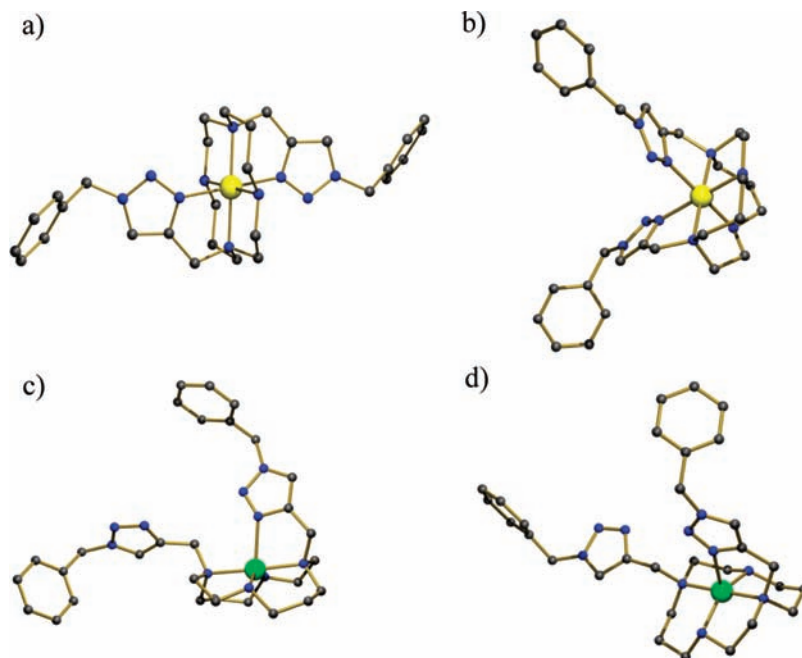
Figure 2. Crystal structures of (a) [Zn(**10**)](ClO$_4$)$_2$, (b) [Ni(**10**)](ClO$_4$)$_2$, (c) [Cu(**10**)](ClO$_4$)$_2$, (d) [Cu(**10**)](PF$_6$)$_2$; a generic atom labeling scheme is presented in Table 2.
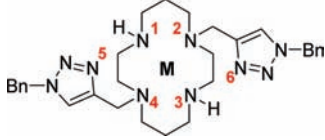
Table 1. X-ray Crystallographic Data^a

|	[Zn(**10**)](ClO$_4$)$_2$	[Ni(**10**)](ClO$_4$)$_2$	[Cu(**10**)](ClO$_4$)$_2$	[Cu(**10**)](PF$_6$)$_2$
empirical formula	C$_{30}$H$_{42}$Cl$_2$N$_{10}$O$_8$Zn	C$_{30}$H$_{42}$Cl$_2$N$_{10}$NiO$_8$	C$_{32}$H$_{45}$Cl$_2$CuN$_{11}$O$_8$	C$_{30}$H$_{42}$CuF$_{12}$N$_{10}$P$_2$1.5C$_7$H$_8$
formula weight	807.01	800.35	846.23	1034.42
crystal size (mm)	0.40 × 0.36 × 0.14	0.22 × 0.12 × 0.06	0.18 × 0.16 × 0.15	0.14 × 0.12 × 0.06
crystal system	monoclinic	monoclinic	triclinic	triclinic
space group	$P2_1/n$	$P2_1/c$	$P1$	$P1$
unit cell dimensions				
a (Å)	10.2539(2)	17.866(2)	10.9250(3)	12.9815(7)
b (Å)	16.8869(5)	10.0482(12)	14.1486(4)	13.1070(6)
c (Å)	11.0525(2) Å	21.869(2)	14.2506(3)	14.3786(7)
α (deg)	90	90	63.385(2)	88.645(3)
β (deg)	115.1890(10)	110.773(5)	77.978(2)	70.461(3)
γ (deg)	90	90	78.005(2)	85.132(3)
volume (Å^3)	1731.83(7)	3670.7(7)	1909.57(9)	2297.3(2)
Z	2	4	2	2
ρ (calcd) (Mg/m^3)	1.548	1.448	1.472	1.495
absorption coefficient (mm^{-1})	0.929	0.736	0.776	0.637
F(000)	840	1672	882	1068
θ range (deg)	3.16−27.50	3.05−27.59	2.93−27.63	2.95−25.00
index ranges	−13 ≤ h ≤ 13	−23 ≤ h ≤ 23	−14 ≤ h ≤ 14	−15 ≤ h ≤ 15
	−21 ≤ k ≤ 21	−13 ≤ k ≤ 13	−18 ≤ k ≤ 18	−15 ≤ k ≤ 15
	−12 ≤ l ≤ 14	−26 ≤ l ≤ 28	−18 ≤ l ≤ 18	−17 ≤ l ≤ 17
reflections collected	22080	29015	34217	32521
independent reflections	3940 [R(int) = 0.0503]	8353 [R(int) = 0.0537]	8724 [R(int) = 0.0532]	8022 [R(int) = 0.0800]
max. and min transmission	0.8810 and 0.7076	0.9572 and 0.8549	0.8925 and 0.8730	0.9628 and 0.9161
data/restraints/parameters	3940/0/220	8353/0/468	8724/0/496	8022/5/569
goodness-of-fit on F^2	1.035	1.087	1.066	1.058
final R indices [$I > 2\sigma(I)$]	R1 = 0.0702, wR2 = 0.1973	R1 = 0.0699, wR2 = 0.1306	R1 = 0.0567, wR2 = 0.1076	R1 = 0.0833, wR2 = 0.1804
R indices (all data)	R1 = 0.0853, wR2 = 0.2087	R1 = 0.1110, wR2 = 0.1530	R1 = 0.0758, wR2 = 0.1175	R1 = 0.1160, wR2 = 0.2060
largest diff. peak and hole (e.Å^{-3})	1.028 and −1.568	0.708 and −0.503	0.626 and −0.459	1.269 and −1.008

^{a} All data were collected using MoKα radiation (λ = 0.71073 Å) at 120(2) K and were refined by full-matrix least-squares on F^2.

titrating a 300 μM solution of Zn(ClO$_4$)$_2$ into a 10 μM solution of **2** (Figure 3) and K_d estimated (because of the very high stability of the complex) as approximately 10^7 M^{-1} (see Supporting Information).[11a] To compare the photophysical properties of **2** with the previously reported

system, the fluorescence of **1** and its response upon the addition of zinc ion were monitored under the same conditions. This revealed the emission intensity of **2** to be roughly double that of **1**, indicating that there are no self-quenching processes taking place between the two fluorophores as
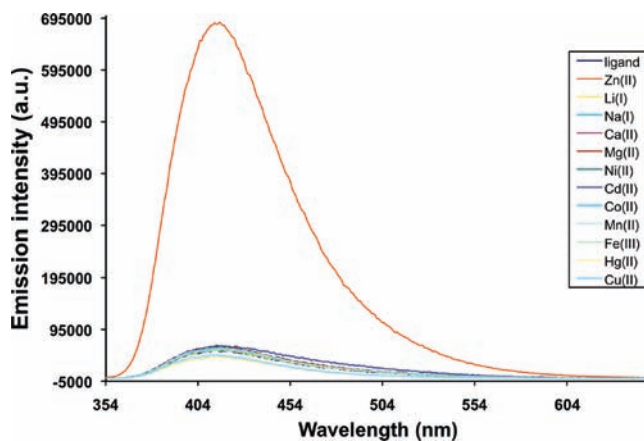
Table 2. Selected Bond Lengths (Å) and Angles (deg) for the Metal Complexes with esds and Schematic Guide to Atom Numbering

	[Zn(10)] (ClO$_4$)$_2$	[Ni(10)] (ClO$_4$)$_2$	[Cu(10)] (ClO$_4$)$_2$	[Cu(10)] (PF$_6$)$_2$
M−N(1)	2.091(3)	2.115(4)	2.021(3)	2.046(5)
M−N(2)	2.158(3)	2.113(2)	2.085(2)	2.076(5)
M−N(3)	2.091(3)	2.071(3)	1.998(3)	2.028(5)
M−N(4)	2.158(3)	2.104(2)	2.070(2)	2.040(5)
M−N(5)	2.217(3)	2.150(3)		
M−N(6)	2.217(3)	2.051(3)	2.274(2)	2.247(5)
N(1)−M−N(5)	88.71(11)	174.19(13)		
N(2)−M−N(5)	100.10(11)	101.80(13)		
N(3)−M−N(5)	91.29(11)	87.01(14)		
N(4)−M−N(5)	79.90(11)	79.67(13)		
N(1)−M−N(6)	91.29(11)	88.62(13)	104.49(10)	103.55(19)
N(2)−M−N(6)	79.90(11)	81.65(13)	79.12(9)	78.81(17)
N(3)−M−N(6)	88.71(11)	172.48(14)	107.14(10)	106.84(19)
N(4)−M−N(6)	100.10(11)	99.18(13)	98.55(9)	99.89(17)
N(5)−M−N(6)	180.00(14)	89.24(13)		
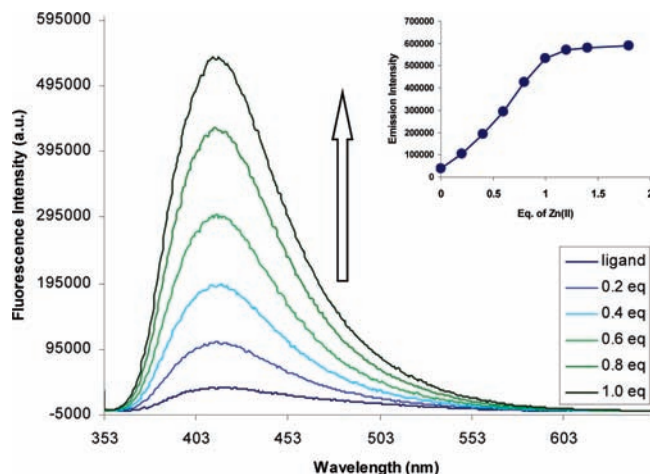
Figure 3. Fluorescence titration of a 10 μM solution of **2** in HEPES buffer/CH$_3$CN (7:3, pH = 7) with a 300 μM solution of Zn(ClO$_4$)$_2$ in water after 25 min. Inset: emission intensity of the solution upon addition of different concentrations of Zn^{2+} (0, 2, 4, 6, 8, 10, 12, 14, and 18 μM). λ_{ex} = 350 nm.

observed for a similar system reported by Valeur et al.[24] in which two identical coumarins were attached to a diaza-18-crown-6.

Structurally related 1,8-disubstituted cyclams derivatized with anthracenes and pyrenes, reported by Chang et al.[25], showed no fluorescence response for Zn(II); the fluorescence response of these systems is extremely sensitive to solvent and generally relies on the quenching of an excimer emission upon binding of certain metal ions to the cyclam ligand, giving a major change in conformation that destroys the excimer. In the case of **2** no self-

(24) Bourson, J.; Pouget, J.; Valeur, B. *J. Phys. Chem.* **1993**, *97*, 4552–4557.

(25) (a) Youn, N. J.; Chang, S.-K. *Tetrahedron Lett.* **2005**, *46*, 125–129. (b) Moon, S.-Y.; Youn, N. J.; Park, S. M.; Chang, S.-K. *J. Org. Chem.* **2005**, *70*, 2394–2397. (c) Park, S. M.; Kim, M. H.; Choe, J.-I.; No, K. T.; Chang, S.-K. *J. Org. Chem.* **2007**, *72*, 3550–3553.

Figure 4. Fluorescence emission of **2** (10 μM) in the presence of a number of other metal ions (10 μM) at pH 7.0 in HEPES buffer/CH$_3$CN 7:3 about 25 min after the addition of the metal ions.

quenching or excimer formation is observed, and we can only speculate that this difference is a result of the reduced conformational flexibility of our system which prevents the two fluorophores engaging in such strong short-range interactions. Thus the coordination of the metal, rather than the dynamic conformation of the ligand, dominates the fluorescence response.
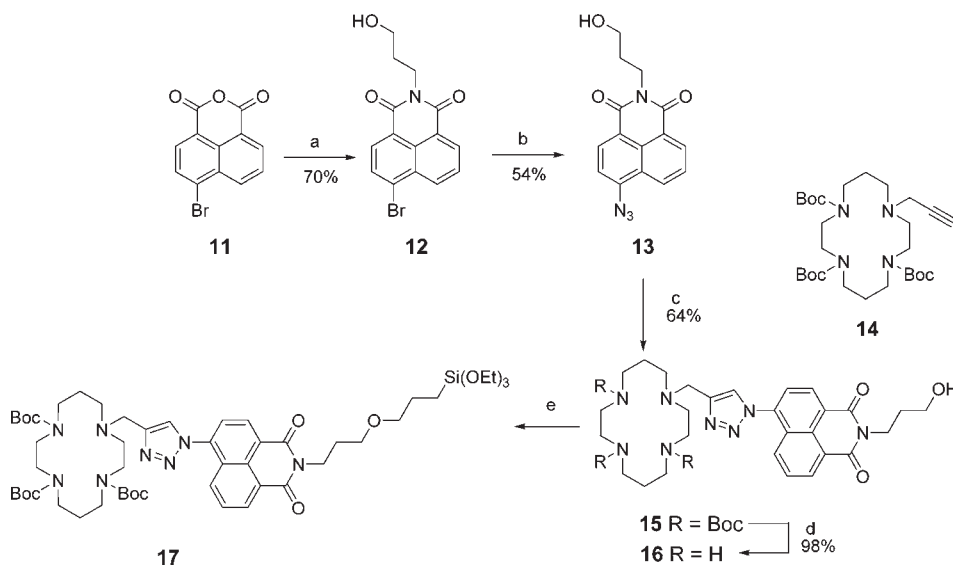
To test the selectivity of **2** for Zn(II), aqueous solutions of a number of other biologically relevant divalent metals were added to a solution of sensor **2** in H$_2$O (HEPES)/CH$_3$CN (7:3). This resulted in a negligible enhancement of the fluorescence emission of the solutions for all of the metals tested (Figure 4). Additionally for Cd(II), selectivity appears to be superior compared to the single fluorophore sensor **1** as the fluorescence of the Cd(II) complex is well within the average response of all of the other metal complexes and is stable at that level for at least 4 h. The emission maximum for Cd(II) does increase slightly after a 24 h period (see Supporting Information) to reach a value which is five times lower than that of the Zn(II) complex, which clearly does not compromise the excellent response selectivity of **2** toward Zn(II). As previously observed for **1**, the fluorescence of **2** is slightly quenched by the addition of Cu(II) and Hg(II), but this is not a concern for potential biological applications of the Zn sensor owing to the very low free intracellular concentrations of these ions.

Competitive binding studies were performed by adding 1 equiv of Zn(II) to solutions of **2** containing a 5-fold excess of competing metal ions after about 25 min. The maximum emission of the solutions before and after the addition of zinc ion were recorded and plotted against the emission intensity of a sample containing [Zn(**2**)]$^{2+}$. Excellent selectivity for Zn(II) over the biologically relevant macro-metals such as Na$^+$, Ca^{2+}, and Mg^{2+} was observed, with the fluorescence of the solution completely restored upon addition of Zn^{2+}, Figure 5. It is evident that **2** also shows exceptional selectivity over most of the first-row transition metals added (Mn^{2+}, Ni^{2+}, Fe^{3+}, and Co^{2+}). Although this selectivity is broadly comparable to that observed for **1** the maximal emission observed for [Zn(**1**)]$^{2+}$ was never recovered in the presence of the transition metal ions, indicating that some of the ligand remained coordinated to the competing metal. In contrast
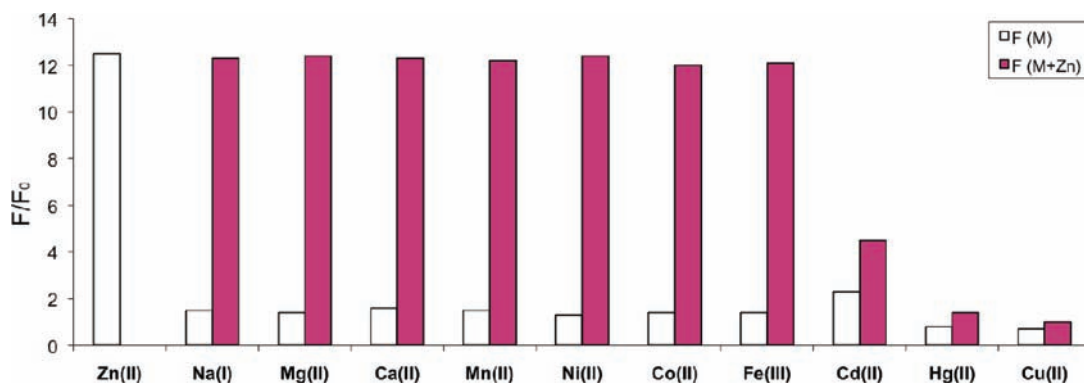
Figure 5. Changes in the fluorescence intensity of **2** upon addition of Zn(II) (10 μM) to a solution of **2** (10 μM) in HEPES buffer/CH$_3$CN (7:3) (pH 7) containing different competing ions (50 μM).

Scheme 2. Synthesis of Sol−Gel Precursor **16**[a]

[a] *Reagent and conditions*: (a) 3-aminopropan-1-ol, dioxane, Δ; (b) NaN$_3$, *N*-pyrrolidinone, Δ; (c) CuSO$_4\cdot$5H$_2$O (5 mol %), Na ascorbate (10 mol %), H$_2$O/THF, rt; (d) TFA (20% in CH$_2$Cl$_2$); (e) NaH, DMF, −20 °C then 3-chloropropyl-triethoxysilane.

for **2** the maximum emission seen for [Zn(**2**)]$^{2+}$ is always recovered. As for **1**, Cd(II), Hg(II), and Cu(II) appear to form such thermodynamically stable complexes with ligand **2** that the addition of Zn(II) to a solution of these complexes only results in a partial increase of the emission intensity of the final mixture. It is therefore apparent that the inherent thermodynamic stability of cyclam complexes is not affected by the incorporation of the two large "click" generated triazole pendant arms and that, as for other putative zinc sensors, application of this system would be limited to common biological environments where the concentrations of Cu(II) are negligible.[17a]

Fabrication of Nanostructured Zinc Sensor Materials. Luminescent chemical sensing by sol−gel derived materials is an attractive area as a result of the versatility and flexibility associated with this method of preparation.[26] The physical properties of these materials, such as stability, optical transparency, flexibility, and permeability are also very appealing, and we viewed ligand systems **1** and **2** as excellent candidates for the generation of such materials. Moreover, the sol−gel process also allows the facile

preparation of a variety of nanostructured materials displaying high surface area-volume ratio using fabrication methods such as soft lithography, electrospinning, and nanopipetting. We were further encouraged by the recent report of the application of siloxane functionalized ligands in the preparation of sol−gel derived silica nanoparticles which were efficacious in the detection of Zn-(II).[27] Given the excellent selectivity for Zn(II) upheld by **1**, the slower complexation rate of Zn(II) by **2**, and the fact that **2** displays only slightly enhanced selectivity/recovery for Zn(II) over other divalent metals over **1** in homogeneous solution, we elected to investigate the efficacy of analogues of **1** as luminescent sol−gel derived materials.

Initially we targeted **17** as a suitable sol−gel precursor as outlined in Scheme 2, as we assumed that Boc deprotection would also occur under the strongly acidic sol−gel conditions employed. Thus, commercially available **11** was readily converted to derivatized alcohol **12** by reaction

(26) Tao, S.; Li, G.; Yin, J. *J. Mater. Chem.* **2007**, *17*, 2730–2736.

(27) Teolato, P.; Rampazzo, E.; Arduini, M.; Mancin, F.; Tecilla, P.; Tonellato, U. *Chem.—Eur. J.* **2007**, *13*, 2238–2245.

(28) Armelao, L.; Bottaro, G.; Quici, S.; Cavazzini, M.; Concetta Raffo, M.; Barigelletti, F.; Accorsi, G. *Chem. Commun.* **2007**, 2911–2913.
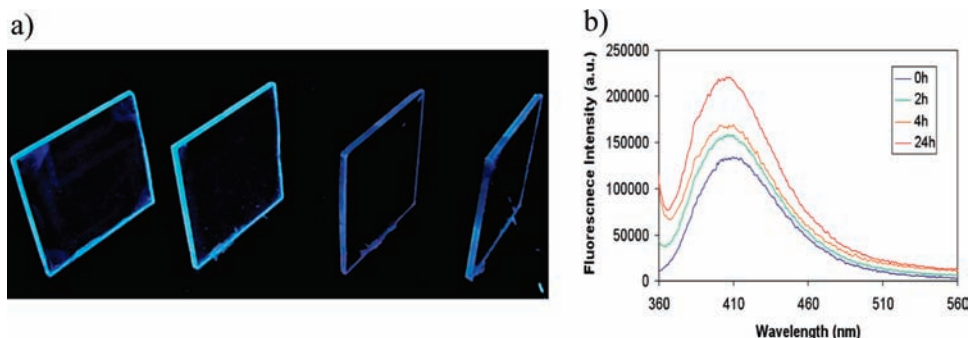
Figure 6. (a) Visualization of the fluorescence response of the sol−gel coated glass slides, and (b) typical fluorescence emission response of the sol−gel coated glass slides upon soaking the coated slides in a 75 μM solution of $ZnSO_4$ for 24 h.

with 3-aminopropan-1-ol in refluxing dioxane overnight. Nucleophilic aromatic substitution with sodium azide, as used to prepare **7**, gave **13** in good overall yield. The click reaction of **13** with the previously reported azide **14** using our standard protocol provided **15** in satisfactory yield. Our attempts to react **15** with (3-chloropropyl)-triethoxysilane provided **17** as judged by NMR spectroscopy, but this material was also contaminated by a number of other unidentified materials. We therefore elected to use the approach recently reported by Barigelletti and co-workers to effect the covalent incorporation of fluorescent molecules into sol−gel matrixes which was reported to produce homogeneous, transparent, and luminescent silica based layers.[29] The global Boc deprotection of **15** proceeded essentially quantitatively using 20% TFA to give **16** which was subsequently incorporated into the siloxane network without further purification under the appropriate processing conditions.

The sol solution was prepared by acid catalyzed copolymerization of tetraethoxysilane in an aqueous/ethanolic medium in the presence of **16**. Sol−gel films were laid by spin-coating the solution onto clean glass substrates at a range of speeds (500−1500 r.p.m.). Following the curing procedure, the derivatized macrocycle was shown to retain its fluorescent response to Zn(II) after soaking the slides in a Zn(II) solution and a representative set of coated glass slides are presented (Figure 6a). The change in fluorescence is evident from Figure 6b; however, longer response times were required with the emission intensity increasing gradually over a period of time, presumably as a result of slower zinc diffusion through the matrix. The detection limit of the films at this stage is about 75 μM Zn(II) as this was the lowest concentration that gave consistent and reproducible results in which a real florescence response rather than noise could be observed.

There are a number of reasonably straightforward methods of overcoming this problem such as enhancing the porosity by variation of the processing conditions or by addition of a co-porogen,[29] which we intend to investigate in due course. However, our aim at this stage was to demonstrate the versatility and ease with which this processing technique could be used in the fabrication

of zinc sensitive micro- and nanostructured materials, such as nanoarrays and nanofibres which have potential for application in devices for the one-off section of zinc. Such structures possess an increased surface to volume ratio, compared with their bulk counterparts, leading to increased accessibility to the recognition sites and thus high sensitivity. For these reasons they should provide materials with improved response times and sensitivity to minute amounts of sample. Furthermore, as such materials can in principle be fabricated into highly ordered arrays we felt that this represented an opportunity to demonstrate the principle of preparation of prototype sensor arrays. On the basis of this we investigated whether nanostructured materials could be prepared by soft lithography,[30] electrospinning,[31] and using a "nanofountain pen"[32] (see Experimental Section). From the images presented in Figure 7 it can clearly be seen that the target materials can be prepared with exquisite control. In the case of the electrospun fibers it proved necessary to add polyethylene oxide to the sol mixture to provide a solution with sufficient viscosity, although alteration of the

(29) (a) Hench, L. L.; West, J. K. *Chem. Rev.* **1990**, *90*, 33–72. (b) Brinker, C. J.; Sehgal, R.; Hietala, S. L.; Deshpande, R.; Smith, D. M.; Loy, D.; Ashley, C. S. *J. Membr. Sci.* **1994**, *94*, 85–102. (c) Boury, B.; Corriu, R. J. P. *Adv. Mater.* **2000**, *12*, 989–992. (d) Flavin, K.; Mullowney, J.; Murphy, B.; Owens, E.; Kirwan, P.; Murphy, K.; Hughes, H.; McLoughlin, P. *Analyst* **2007**, *132*, 224–229.

(30) (a) Xia, Y. N.; Whitesides, G. M. *Annu. Rev. Mater. Sci.* **1998**, *28*, 153–184. (b) Xia, Y. N.; Whitesides, G. M. *Angew. Chem., Int. Ed.* **1998**, *37*, 551–575.

(31) (a) Doshi, J.; Reneker, D. H. *J. Electrostatics* **1995**, *35*, 151–160. (b) Li, D.; Xia, Y. N. *Adv. Mater.* **2004**, *16*, 1151–1170.

(32) Belmont, A.-S.; Sokuler, M.; Haupt, K.; Gheber, L. A. *Appl. Phys. Lett.* **2007**, *90*, 193101.

(33) Hooft, R. *Collect: Data collection software*; Nonius B.V.: Delft, The Netherlands, 1998.

(34) Otwinowski, Z.; Minor, W. *Denzo, data collection and processing software*. In *Methods in Enzymology*; Carter, C. W., Jr., Sweet R. M., Eds.; Academic Press: New York, 1997; Macromolecular Crystallography, part A, Vol. 276, pp307−326.

(35) *MaXus solution and refinement software suite*; Mackay, S.; Gilmore, C. J.; Edwards, C.; Tremayne, M.; Stewart, N.; Shankland, K.

(36) *SORTAV, absorption correction software package*; Blessing, R. H. *Acta Crystallogr.* **1995**, *A51*, 33−37 and Blessing, R. H. *J. Appl. Crystallogr.* **1997**, *30*, 421−426.

(37) Beurskens, P. T.; Beurskens, G.; Bosman, W. P.; de Gelder, R.; Garcia-Granda, S.; Gould, R. O.; Israel, R.; Smits, J. M. M. *DIRDIF99 program system*; Crystallography Laboratory, University of Nijmegen: The Netherlands, 1999.
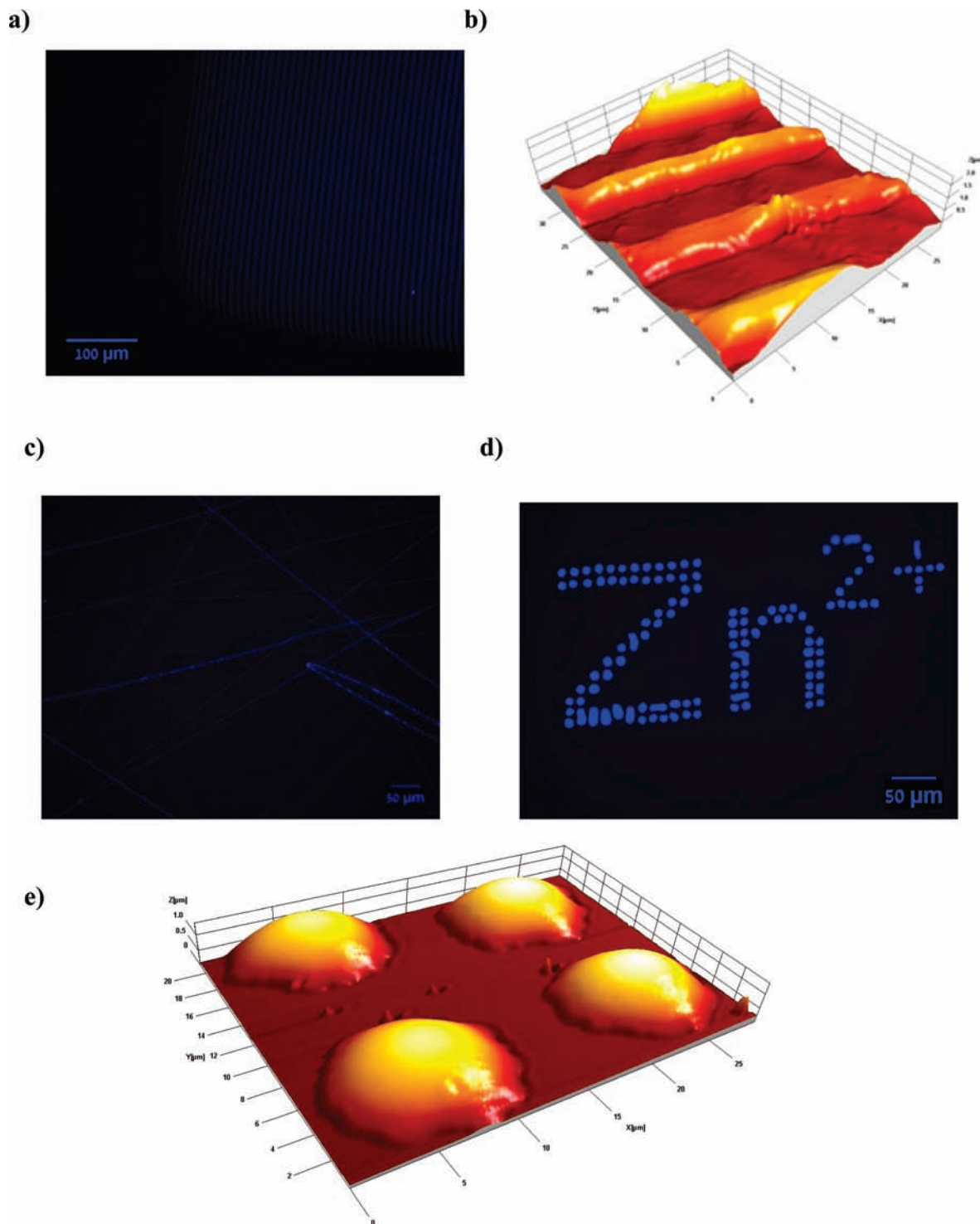
(38) Sheldrick, G. M. *SHELX97 [Includes SHELXS97, SHELXL97, CIFTAB (and SHELXA)]* - *Programs for Crystal Structure Analysis*, Release 97−2; Institüt für Anorganische Chemie der Universität: Göttingen, Germany, 1998.

(39) *ORTEP3 for Windows*; Farrugia, L. J. *J. Appl. Crystallogr.* **1997**, *30*, 565.

(40) (a) *PLATON/PLUTON*; Spek, A. L. *Acta Crystallogr., Sect. A* **1990**, *46*, C34. (b) Spek, A. L. *PLATON, A Multipurpose Crystallographic Tool*; Utrecht University: Utrecht, The Netherlands, 1998.

(41) WINGX, Farrugia, L. J. *J. Appl. Crystallogr.* **1999**, *32*, 837−838.

Figure 7. Sol−gel nanostructures fabricated from **16** prepared using (a, b) soft lithography, (c) by electrospinning, and (d, e) by nanofountain pen, visualized by fluorescence microscopy (a, c, and d) and AFM (b and e).

processing conditions should allow the direct use spinning of the sol-solution in the absence of any additives.[29]

Conclusions

We have reported the synthesis of a new class of cyclam-based "clickates" capable of the selective detection of Zn(II) over a number of other divalent metals which provides a 2-fold increase in the fluorescence response compared to our previously reported system **1**. The selectivity of this ligand system for binding Zn(II) is comparable to the best PET based zinc sensors reported to date. This is reflected in competitive binding experiments with a range of metal cations, which also show almost complete recovery of the maximal fluorescent response. As is the case for many putative zinc sensors in the presence of an excess of Cu(II), Hg(II), and Cd(II), the addition of Zn(II) results in only a small recovery of fluorescence. For the majority of biological applications such deficiencies are not important as neither

Hg(II) nor Cd(II) occur in significant concentrations in biology, and it has been recently estimated that free Cu(II) is limited to less than one free Cu(II) atom per cell.[17a] Nonetheless, in cases where Cu(II) concentrations are comparable to Zn(II), for example, in amyloid plaques,[17b] further developments are required to improve sensor selectivities. Although the response of the new ligands was superior to **1** in that it provided an enhanced fluorescence response and improved recovery of fluorescence in the presence of other divalent metals, its response to zinc was significantly slower. We therefore chose to prepare sol−gel derived materials using a derivative of ligand **1** and demonstrated that the sol−gel material retains its sensitivity for Zn(II). We also show in a proof of principle study that the sol−gel precursor **16** can be used in the fabrication of a range of highly ordered nanostructured materials. As a result of these finding we propose that it will be possible to prepare highly structured nanoarrays for the selective detection, and ultimately quantitation, of zinc in vivo and in vitro. Investigations along these lines are currently ongoing in our laboratories.

Supporting Information Available: Figures S1−S27, Tables S1 and S2, and crystallographic data in the form of CIF files. This material is available free of charge via the Internet at http://pubs.acs.org.